Max-Planck-Institut für Meteorologie
Max Planck Institute for Meteorology

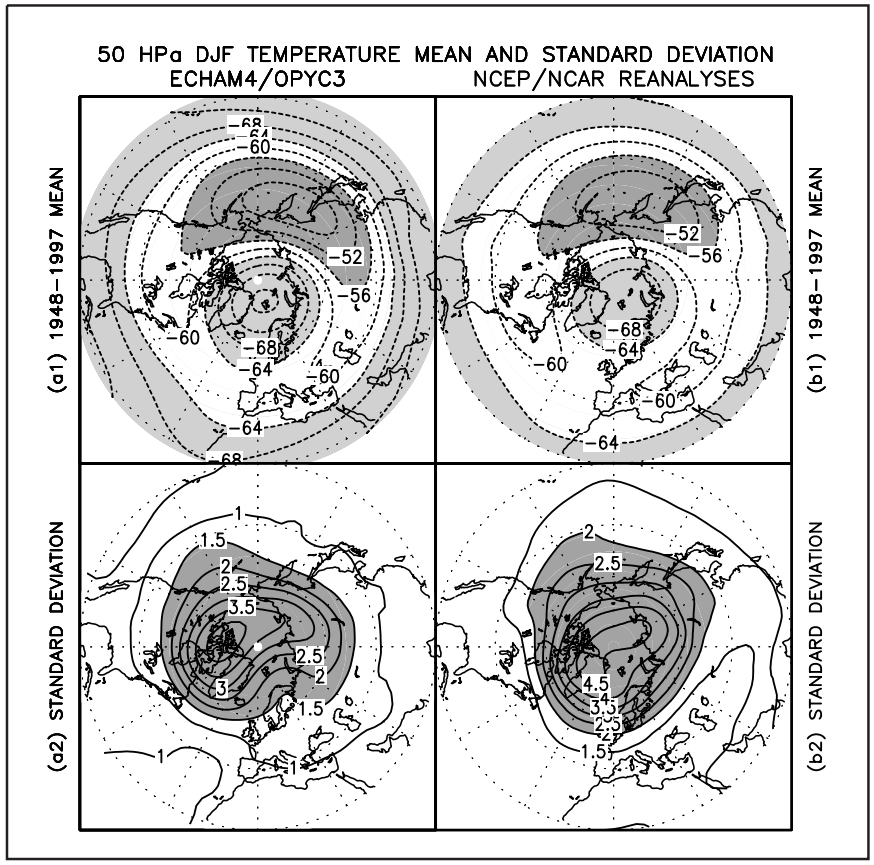

Stratospheric Response to Global Warming in the Northern Hemisphere Winter

by

Zeng-Zhen Hu

Hamburg, November 2001

Authors

Zeng-Zhen Hu Max-Planck Institut für Meteorologie

Max-Planck-Institut für Meteorologie
Bundesstrasse 55
D - 20146 Hamburg
Germany

Tel.: +49-(0)40-4 11 73-0
Fax: +49-(0)40-4 11 73-298
e-mail: <name>@dkrz.de
Web: www.mpimet.mpg.de

Stratospheric Response to Global Warming in the Northern Hemisphere Winter

Zeng-Zhen Hu

Max-Planck-Institut für Meteorologie
Bundesstrasse 55, D-20146 Hamburg, Germany

present affiliation:
Center for Ocean-Land-Atmosphere Studies
Calverton, Maryland 20705, USA

ISSN 0937 - 1060

Abstract

Lower stratospheric climate response to global warming in the Northern Hemisphere winter was investigated by a transient greenhouse warming integration with the ECHAM4/OPYC3 coupled global climate model. The dynamics of the response was studied through analyses of kinetic energy of various wavenumbers, vertical propagation of planetary waves, and feedback between transient eddy activity and the zonal mean circulation. It is indicated that the zonal mean circulation, especially at high latitudes and subtropics, becomes stronger in the upper troposphere (300 hPa) than in the current climate, mainly associated with a significant intensification of the meridional temperature gradient. In the lower stratosphere (50 hPa), a cooling occurs with a stronger polar night jet. The kinetic energy in the upper troposphere decreases for wave number 2 and increases for wave number 1. The stratospheric cooling is further enhanced because of a reduction in the vertical wave energy propagation from the troposphere to the stratosphere, which is the result of the zonal mean wind and kinetic energy changes, thus acting as a positive feedback mechanism. In addition, transient eddy activity plays a positive role in the zonal mean wind change in the upper troposphere at increased greenhouse gas forcing.

1. Introduction

The annual global surface temperature has increased by about 0.6-0.7°C over the recent 100 years and a marked warming has taken place since the end of 1970s (Jones et al., 1999; Hansen et al., 1999). Impact of human activities on the global climate and the environment has become a widespread concern (WCRP, 1998). In the stratosphere, model experiments have shown a marked cooling in addition to the tropospheric warming at increased greenhouse gas forcing (Manabe and Wetherald, 1975). The stratosphere climate response to greenhouse gases and the interaction between the response and the stratospheric chemical reactions are attracting increased scientific interest. For example, with a series of numerical experiments of the ECHAM4/OPYC3 model, Bengtsson et al. (1999) demonstrated that the reduction of the stratospheric ozone does not only cool the lower stratosphere but also the troposphere, in particular the upper and middle parts, thus counteracting the greenhouse effect. A number of studies have also suggested that increased CO_2 and other greenhouse gases could also affect Arctic ozone. Austin et al. (1992) predicted the possibility of an Arctic ozone hole in a double CO_2 experiment based on 3-D model calculations. With sensitivity studies using a box model for an idealized parcel, Danilin et al. (1998) indicated that the stratospheric cooling could further deplete ozone via increased polar stratospheric cloud formation and thus delay its expected recovery. The work of Shindell et al. (1998) argues for a key role for such a feedback both in the 1990s and perhaps in the future years, with the peak

Arctic ozone losses being predicted to occur near 2010. Thus, the tropospheric warming and the stratospheric ozone hole and the chemical reaction seem physically connected. It is interesting to probe the physical mechanism behind the connection.

The role of the upper tropospheric and lower stratospheric atmosphere response to greenhouse warming seems more complex and more important than expected. It is therefore of interest to further elucidate these questions with a different climate model. In this work we investigate the upper tropospheric and lower stratospheric climate response to increased greenhouse gas forcing in the Northern Hemisphere (NH) winter on the basis of a transient integration. In Section 2 the coupled model, the experiment, and the data are briefly described. Sections 3 and 4 show the responses of the upper tropospheric and lower stratospheric large-scale atmospheric circulation to the greenhouse warming and their dynamical connection, respectively. Conclusions and discussions are given in Section 5.

2. Model, experiment and data

The model used in this study is the ECHAM4/OPYC3 coupled model. The atmosphere model (ECHAM4) is a spectral model with triangular truncation of total horizontal wavenumber 42 (T42). The OGCM component (OPYC3) consists of three submodels; the interior ocean, the surface mixed layer and the sea ice, respectively. The ECHAM4 and OPYC3 are coupled synchroneously with an exchange of information once a day. Fluxes of momentum are unconstrained, while fluxes of heat and fresh water are flux adjusted but only by annual averages. The detailed description of the ECHAM4 and OPYC3 models can be found in Roeckner et al. (1996, and references therein) and Oberhuber (1993), respectively. The detailed coupling strategy and technology of ECHAM4 and OPYC3 are described by Bacher et al. (1998). The experiment of the ECHAM4/OPYC3 is a 240 year (1860-2100) simulation of transient greenhouse warming (GHG). In the GHG run, from 1860 to 1990, the annual concentrations of the well mixed greenhouse gases (CO_2, N_2O, CH_4, and CFCs) are prescribed as observed and, from 1990 onwards, according to IPCC scenario IS92a (IPCC, 1992). Details can be found in Roeckner et al. (1999).

The ECHAM4/OPYC3 has been thoroughly evaluated in extensive control integrations (Christoph et al., 1998; Bacher et al., 1998) and global warming run (Jin et al., 2001; Hu et al., 2000a, 2000b, 2001; Latif et al., 2000; Roeckner et al., 1999; Bengtsson, 1999). It has been demonstrated that the ECHAM4/OPYC3 reasonably well simulates the present climate in the troposphere and its variability. Comparison with the NCEP/NCAR reanalyses (Kalnay, et al., 1996) and the GHG run, it is demonstrated that the ECHAM4/OPYC3 considerably well simulates the spatial distribution and temporal evolution of the large-scale atmospheric circulation in the upper troposphere and lower

stratosphere, including the annual cycle, climatological mean, and variance. Fig. 1 is an example, which shows that the climatological mean of 50 years and standard deviations of the winter (DJF) temperature at 50 hPa are well simulated by the ECHAM4/OPYC3, although the standard deviations are somewhat underestimated in the model. Recently, with another coupled model (ECHAM4/LSG), Perlwitz et al. (2000) demonstrated that the vertical propagation of the stationary waves and the leading variability modes of the coupled troposphere-stratosphere winter circulation in the high latitudes and polar region are well simulated by the model. Therefore, with the GHG run it is reasonable to analyze the upper tropospheric and lower stratospheric climate response to the increase of the greenhouse gas concentrations and the dynamical connection between the responses.

Seasonal mean of temperature and horizontal component of wind at 300 hPa and 50 hPa in DJF are used to represent the upper troposphere (tropopause) and lower stratosphere, respectively. The analysis is confined to the NH and focused on the linear trends 1990-2100 and the differences between the 50 year means of 1860-1910 and 2050-2100. The period 2050-2100 is defined as the transient GHG scenario period with significant increase of GHG, and the period 1860-1910 as the reference period without significant increase of GHG. The decadal (10 years) averages (1980-1990, 2030-2040, 2070-2080, and 2090-2100) of the localized Eliassen-Palm flux at 300 hPa and its divergence in winter are used to identify the role of the transient eddy activity on the variation of zonal mean circulation in the upper troposphere.

3. Changes in the large-scale atmosphere circulation

3.1 Temperature and wind at 300 hPa

For the time-evolution of the temperature at 300 hPa (T300) averaged in the NH, there is a clear warming trend from the 1990s onward (not shown). The warming trend follows the increase of the greenhouse gas forcing. Fig. 2a shows the two-dimensional distributions of the linear trends of T300 from 1990 to 2100, which are calculated based on the linear regression. According to a t-test, the warming trends are significant everywhere at the 99% level. The amplitudes of the trends are larger at lower latitudes than at higher latitudes. The large warming occurs in the tropics with values greater than 0.6°C/decade. This kind of trend distribution leads to an increase in the meridional temperature gradient, especially at the latitudes of 20°N-40°N (Fig. 3a).

The variability of the averaged zonal wind at 300 hPa (U300) is stable until the year of 2000, then a upward trends become pronounced (not shown). The positive significant trends at the 99% level occur mainly in two latitude bands (Figs. 2b, 3b). One is at 50°N-65°N, and the other is at 15°N-30°N. The linear trends of U300 at 15°N-30°N are mainly due to the increase of the meridional temperature gradient at these latitudes, as shown in Figs. 2a and 3a, through the thermal wind relation, since the slope of the curve

of the zonal mean T300 at 20°N-35°N is sharper in 2050-2100 than in the reference period 1860-1910 (Fig. 3a). The linear trends of U300 at 50°N-65°N (Figs. 2b, 3b) are mainly the result of a dynamical feedback of the atmosphere to the global warming as shown in the next section.

3.2 Temperature and wind at 50 hPa

In contrast to the warming trend at 300 hPa, a cooling trend takes place at 50 hPa (T50) and becomes evident after the 1970s (not shown). The amplitude of the cooling is 3.5°C by the year of 2100. Fig. 4a shows the two-dimensional distributions of linear trends of T50 over the NH in 1990-2100. The cooling trends are greater than 1.0°C/decade in the regions north of 70°N. There are also cooling trends in the tropics. Warming trends are pronounced at temperate latitudes with maximum values greater than 0.3°C/decade. The cooling and the warming trends are significant at the 99% level. According to the zonal means (Fig. 5a), the cooling exists mainly at high latitudes and in the tropics, while warming is found at temperate latitudes. The mean amplitudes of the cooling in the regions north of 70°N are about 10°C by 2100 (not shown).

The increase of the zonal wind (U50) is also noticeable, particularly after the 1980s with amplitudes in range of 5-6 m/s by the year of 2100 (not shown). A general increase of U50 is clearly demonstrated in two-dimensional distributions of the linear trends of U50 over the NH in 1990-2100 (Fig. 4b) and also in the zonal mean of U50 (Fig. 5b). Most of the positive trends in Fig. 4b are significant at the level of 99% in the T-test. The largest accelerations are greater than 1.4 m/s/decade (Fig. 4b). The pronounced positive accelerations are mainly at 20˚N-70˚N (Fig. 5b), especially in regions from East Siberia to the North Pacific (Fig. 4b), which cohere with the intensified temperature gradient there shown in Fig. 4a. This distribution of U50 makes the polar circulation become more symmetric relative to the North Pole. In addition, the negative trends of U50 in the tropics are also significant (Fig. 4b).

4. Dynamical connection

This section is focused on kinetic energy change for different wave numbers in the global warming scenario and impact of the global warming on vertical propagation of the planetary waves. The role of transient eddies in affecting the zonal mean state is also investigated through analyzing the localized Eliassen-Palm flux and its divergence in different periods of the GHG run.

wave numbers	2050-2100	1860-1910	<2050-2100> - <1860-1910>
zonal mean	293.2	263.1	30.1 (11%)*
1	17.7	13.4	4.3 (32%)*
2	7.8	12.4	-4.6 (-37%)**
3	8.8	8.1	0.7 (8%)
4	2.4	2.3	0.1 (5%)
5	0.4	0.5	-0.1 (-24%)

Table 1: Kinetic energy of U300 for the zonal mean and wave numbers 1- 5 averaged over the latitudes of 55˚N-65˚N during 1860-1910 and 2050-2100 and their differences in winter. The differences with * and ** are significant at the level of 90% and 99 % using the t-test, respectively. The unit is m^2/s^2. Values in the brackets are the relative differences in %.

4.1 Kinetic energy

The kinetic energy is analyzed for 50-year winter mean U300 averaged over high latitudes (55˚N-65˚N chosen as a representative) during 1860-1910 and 2050-2100. The corresponding values for zonal mean U300 and wave numbers 1-5 and their differences are listed in Table 1. It is shown that the kinetic energy of the winter mean circulation in the upper troposphere is concentrated in the first 4 longest waves. The kinetic energy increases by 11 % for the zonal mean U300 and 32 % for wave number 1 (Table 1). The enhancement of the kinetic energy for the zonal mean U300 is coherent with the intensification of the zonal mean U300 at 55˚N-65˚N in 2050-2100, and also with the linear trends of U300 in Fig. 2b and the zonal mean of U300 in Fig. 3b. The most significant change of the kinetic energy is the decrease for wave number 2 in 2050-2100 in comparison with that in 1860-1910. The decrease indicates that dipole-like polar circulations become less frequent while symmetric circulations at high latitudes relatively to the North Pole become more frequent in the global warming scenario. A symmetric circulation at the upper troposphere is unfavorable for the vertical propagation of planetary waves from the troposphere to the stratosphere and for the occurrence of stratosphere sudden warming.

4.2 Vertical propagation of the planetary waves

The stratospheric circulation is influenced by the upward propagation of the forced planetary waves in the troposphere. The forced planetary waves play a crucial role in the dynamics of the stratospheric sudden warming, based on current theories, first proposed by Matsuno (1971). The vertical propagation of the forced planetary waves occurs in a certain condition which is associated with the U component of wind. The global warming alters the general circulation at 300 hPa, thus it is expected that the vertical

propagation of the forced planetary waves will be affected. The impact of global warming on the upward propagation of the forced planetary waves in the upper troposphere is qualitatively investigated according to the theory of Charney and Drazin (1961).

Let the motion be referred to a *ß*- plane centered at 60˚N, scale height H= 7 km, infinite meridional scale (l=0), and for a typical stratospheric static stability and buoyancy frequency $N=2.0*10^{-2}s^{-1}$, the Rossby critical velocities $U_c = ß/((k^2+l^2)+f_0^2/(4N^2H^2))$ for zonal wave numbers of 1, 2, and 3 are calculated and shown in Fig. 6. The vertical propagation of planetary waves can occur only in the presence of westerly winds weaker than a critical value that depends on the horizontal scale of the waves, i. e., in the region of $0< \bar{u} <U_c$ (Charney and Drazin, 1961; Holton, 1992). Fig. 6 indicates the impact of the increased greenhouse gas concentrations on the vertical propagation of the planetary waves. With the enhancement of the zonal mean U300 at 55°N-65°N in 2050-2100, the 'window' for the propagation of the planetary waves becomes smaller in 2050-2100 than in 1860-1910. The upward propagation of planetary waves from the troposphere to the stratosphere is restrained under increased greenhouse forcing. This is consistent with the circulation change analyzed in Section 3.1 and the kinetic energy change studied in the previous subsection.

In the global warming scenario, the polar circulation in the upper troposphere becomes stronger (Figs. 2, 3), and the gradient of the temperature at 50 hPa between 50˚N and 85˚N increases obviously (Figs. 4, 5), which seems associated with less frequent stratospheric sudden warming (Labitzke, 1984). This agrees with the result of the restrained vertical propagation of the planetary waves from the troposphere to the stratosphere in 2050-2100. As a consequence of less vertical propagation of planetary waves, further cooling occurs in the Arctic, leading to a strengthening of the polar circulation at the stratosphere. This is a positive feedback, which is coherent with the analyses in Section 3 and Shindell et al. (1998). The mechanism suggested by Shindell et al. (1998) is that cooling in the stratosphere caused by increased greenhouse gas forcing is associated with a more pronounced polar vortex in the lower stratosphere and upper troposphere, which reduces the vertical wave propagation through the tropopause and hence leads to a further acceleration of the chemical destruction of ozone at high latitudes due to increased cooling of the Arctic stratosphere.

4.3 Localized Eliassen-Palm flux

Transient eddy activity is basically determined by the stationary state, but there is also a feedback of the transient eddy activity on the stationary state (Lau and Holopainen, 1984). Through this feedback, the transient eddy activity can alter the stationary state. The localized Eliassen-Palm flux and its divergence are a good measure of the feedback (Trenberth, 1986). In this subsection we focus on the zonal component of wind and use

the localized Eliassen-Palm flux and its divergence as diagnostics of the eddy forcing of the zonal flow at 300 hPa. With a 2-6 day bandpass filter (Press et al., 1989), winter means of the zonal component of two-dimensional (latitudinal and longitudinal) localized Eliassen-Palm flux ($E_u = [(\overline{v'^2} - \overline{u'^2})/2, -\overline{u'v'}]$) and its divergence ($\nabla \cdot E_u$) at 300 hPa are calculated according to the definition given by Trenberth (1986), where u' and v' are the transient components of daily data with the 2-6 day bandpass filter, and $\overline{u'^2}$, $\overline{v'^2}$, and $\overline{u'v'}$ represent the winter means.

Changes of the localized Eliassen-Palm flux and its divergence for various periods in the GHG run are confined in the regions associated with the storm tracks in the NH (not shown). From the zonal mean of the localized Eliassen-Palm flux divergence in Fig. 7, a noticeable poleward shift of the maximum value is found from 1980-1990, a period without significant warming, to three later periods with significant warming. The maximum divergence zone moves from 35˚N-40˚N in 1980-1990 to 55˚N-60˚N in the other periods (Fig. 7). The convergence of the localized Eliassen-Palm flux at 25˚N-30˚N is also noticeable. However, both the position and intensity changes are less pronounced in the later decades. The impact of the global warming on the localized Eliassen-Palm flux convergence and on the westerly deceleration of the zonal mean flow at 25˚N-30˚N is less significant (Figs. 6, 7).

The northward shift of the maximum divergence zone indicates that the transient eddy activity speeds up the westerlies at 50˚N-60˚N. This is confirmed by the time-evolution of zonal mean U300 anomalies (Fig. 8). Two positive and one negative anomaly belts are dominant in the significant warming periods, which agrees with Figs. 2b and 3b. One positive belt is at 50˚N-65˚N with maxima of 1.5 m/s (Fig. 8) since the year of 2040, which is related to the transient activity forcing (Fig. 7). The enhanced U300 in 50˚N-60˚N retards upwelling planetary wave activity from the troposphere to the stratosphere. The other positive belt is at 10˚N-30˚N with maxima of 2.1 m/s (Fig. 8). As the convergences of the localized Eliassen-Palm fluxes at 10˚N-35˚N (Fig. 7) reduce the west wind component it follows that the positive anomalies of U300 at 10˚N-30˚N (Fig. 8) must be caused by the temperature gradient changes as shown in Figs. 2a and 3a. This analysis demonstrates that the transient eddy activity plays an active role in the zonal wind change in the upper troposphere.

5. Conclusions and discussions

The upper tropospheric and lower stratospheric climate responses to the global warming in the Northern Hemisphere winter were investigated in a transient greenhouse warming integration with the ECHAM4/OPYC3 model. The dynamical aspect was studied through analyses of the impact of the global warming on kinetic energy of various wave

numbers, vertical propagation of the planetary waves, and the feedback of transient eddy activity on the mean zonal circulation.

The increased greenhouse gas concentrations lead to a general warming of the troposphere, most pronounced in its upper part. The zonal mean circulation at 300hPa is increasing somewhat at high latitudes and in the subtropics as a consequence of the enhanced meridional temperature gradient and non-linear eddy transfer. At 50 hPa a general cooling takes place, in particular at high latitudes. The band of higher temperatures at mid latitudes is presumably caused by changes in the meridional circulation. The zonal wind at 50 hPa is successively strengthening, generating a major increase of the zonal circulation towards the end of the 21st century.

Typical changes also occur in the kinetic energy spectrum. In the upper troposphere, there is a marked increase in the zonal mean component and in wave number 1 and a pronounced decrease in wave number 2. The energy change of shorter wave components are minor and not significant. The change in the wave spectrum towards longer waves restricts the vertical energy propagation from the troposphere into the stratosphere. This is in agreement with the investigation by Perlwitz et al. (2000) and shows that the transient eddy activity plays a active role in the zonal wind changes. As a result, additional cooling occurs in the Arctic and the zonal mean circulation and the polar night jet are further enhanced. This positive feedback is consistent with the mechanism put forward by Shindell et al. (1998). However, it should be stressed that the interaction with stratospheric chemistry and ozone is not considered here, a process which could enhance the change in the circulation even further.

As the vertical component of the E-P flux and daily data are unavailable, the impact of global warming on the vertical propagation of the planetary waves can only be shown qualitatively by calculating the changes of the kinetic energy and the Rossby critical velocity. The impact of global warming on the frequency of stratospheric sudden warming events is another aspect to be investigated. The influence of the coarse vertical resolution in the stratosphere with an upper boundary at 10 hPa is a limiting factor as is the lack of interaction with atmospheric chemistry. We intend to consider these aspects in future investigations.

Acknowledgments

The authors are grateful to the colleagues at MPI for Meteorology and F.-F. Jin for their valuable comments, suggestions and encouragement. Special thanks are due to M. Christoph for his kind supply of the bandpass data and helpful discussion. The Figures in this article were prepared using the graphics software GrADS, developed by Brian Doty of COLA/IGES. At COLA, the first author was supported by NSF grant ATM9907915.

References

Austin, J., Butchart, N. and Shine, K. P. 1992. Possibility of an Arctic ozone hole in a doubled-CO_2 climate. *Nature* **360,** 221-225.

Bacher, A., Oberhuber, J. M. and Roeckner, E. 1998. ENSO dynamics and seasonal cycle in the tropical Pacific as simulated by the ECHAM4/OPYC3 coupled general circulation model. *Clim. Dyn.* **14,** 431-450.

Bengtsson, L. 1999. Numerical modelling of the Earth's climate. In: *Modeling the Earth's Climate and its Variability* (eds. Holland, W. R., Joussaume, S. and David, F.) Elsevier Science. 139-235.

Bengtsson, L., Roeckner, E. and Stendel, M. 1999. Why is the global warming proceeding much slower than expected ? *J. Geophys. Res.* **104**, 3865-3876.

Charney, J. G. and Drazin, P. G. 1961. Propagation of planetary scale disturbances from the lower into the upper atmosphere. *J. Geophys. Res.* **66**, 83-109.

Christoph, M., Barnett, T. P. and Roeckner, E. 1998. The Antarctic circumpolar wave in a coupled ocean-atmosphere GCM. *J. Clim.* **11**, 1659-1672.

Danilin, M. Y., Sze, N.-D., Ko, M. K. W., Rodriguez, J. M. and Tabazadeh, A. 1998. Stratospheric cooling and Arctic ozone recovery. *Geophys. Res. Lett.* **25**, 2141-2144.

Hansen, J., Ruedy, R., Glascoe, J. and M. Sato, 1999. GISS analysis of surface temperature change. *J. Geophys. Res.* **104**, 30997-31022.

Holton, J. R. 1992. *An Introduction to Dynamic Meteorology (Third Edition)*. Academic Press, Inc., California, 511 pp.

Hu, Z.-Z., Bengtsson, L., Roeckner, E., Christoph, M., Bacher, A. and Oberhuber, J. M. 2001. Impact of global warming on the interannual and interdecadal climate modes in a coupled GCM. *Clim. Dyn.* **17,** 361-374.

Hu, Z.-Z., Bengtsson, L. and Arpe, K. 2000a. Impact of global warming on the Asian winter monsoon in a coupled GCM. *J. Geophys. Res.* **105**, 4607-4624.

Hu, Z.-Z., Latif, M., Roeckner, E. and Bengtsson, L. 2000b. Intensified Asian summer monsoon and its variability in a coupled model forced by increasing greenhouse gas concentrations. *Geophys. Res. Lett.* **27**, 2681-2684.

IPCC (Intergovernmental Panel on Climate Change), 1992. *Climate Change 1992. The Supplementary Report to the IPCC Scientific Assessment* (eds. Houghton, J. T., Callander, B. A. and Varney, S. K. V.) Cambridge University Press, Cambridge, 198 pp.

Jin, F.-F., Hu, Z.-Z., Latif, M., Bengtsson, L. and Roeckner, E. 2001. Dynamics and cloud-radiation feedbacks in El Niño and greenhouse warming. *Geophys. Res. Lett.* **28**, 1539-1542.

Jones, P. D., New, M., Parker, D. E., Martin, S. and Rigor, I. G. 1999. Surface air temperature and its changes over the past 150 years. *Rev. Geophys.* **37**, 173-199.

Kalnay, E., Kanamitsu, M., Kistler, R., Collins, W., Deaven, D., Gandin, L., Iredell, M., Saha, S., White, G., Woollen, J., Zhu, Y., Chelliah, M., Ebisuzaki, W., Higgins, W., Janowiak, J., Mo, K. C., Ropelewski, C., Wang, J., Leetmaa, A., Reynolds, R., Jenne, R. and Joseph, D. 1996. The NCEP/NCAR 40-year reanalysis project. *Bull. Am. Meteor. Soc.* **77**, 437-471.

Labitzke, K. 1984. Stratospheric-mesospheric midwinter disturbances: A summary of observed characteristics. *J. Geophys. Res.* **89**, 9665-9675.

Latif, M., Roeckner, E., Mikolajewicz, U. and Voss, R. 2000. Tropical stabilization of the thermohaline circulation in a greenhouse warming simulation. *J. Clim.* **13**, 1809-1813.

Lau, N.-C. and Holopainen, E. O. 1984. Transient eddy forcing of the time-mean flow as identified by geopotential tendencies. *J. Atmos. Sci.* **41**, 313-328.

Manabe, S. and R. T. Wetherald, R. T. 1975. The effect of doubling CO_2 concentration on the climate of a GCM. *J. Atmos. Sci.* **32**, 3-15.

Matsuno, T. 1971. A dynamical model of the stratospheric sudden warming. *J. Atmos. Sci.* **28**, 1479-1494.

Oberhuber, J. M. 1993. Simulation of the Atlantic circulation with a coupled sea-ice-mixed layer-isopycnal general circulation model. Part I: Model description. *J. Phys. Oceanogr.* **23**, 808-829.

Perlwitz, J., Graf, H.-F. and Voss, R. 2000. The leading variability mode of the coupled troposphere-stratosphere winter circulation in different climate regimes. *J. Geophys. Res.* **105**, 6915-6926.

Press, W. H., Flannery, B. P., Teukolsky, S. A. and Vetterling, W. T. 1989. *Numerical Recipes*. Cambridge University Press, Cambridge, 702 pp.

Roeckner, E., Arpe, K., Bengtsson, L., Christoph, M., Claussen, M., Dümenil, L., Esch, M., Giorgetta, M., Schlese, U. and Schulzweida, U. 1996. The atmospheric general circulation model ECHAM-4: Model description and simulation of present-day climate. *Max-Planck-Institut für Meteorologie Report* **218**, 1-90.

Roeckner, E., Bengtsson, L., Feichter, J., Lelieveld, L. and Rodhe, H. 1999. Transient climate change simulations with a coupled atmosphere-ocean GCM including the tropospheric sulfur cycle. *J. Clim.* **22**, 3004-3032.

Shindell, D. T., Rind, D. and Lonergan, P. 1998. Increased polar stratospheric ozone losses and delayed eventual recovery owing to increasing greenhouse-gas concentrations. *Nature* **392**, 589-592.

Trenberth, K. E. 1986. An assessment of the impact of transient eddies on the zonal flow during a blocking episode using localized Eliassen-Palm flux diagnostics. *J. Atmos. Sci.* **43**, 2070-2087.

WCRP (World Climate Research Programme), 1998. *CLIVAR Initial Implementation Plan.,* WCRP **No. 103,** WMO/TD **No. 869,** ICPO **No. 14,** World Meteorological Organization, Geneva, 1-314.

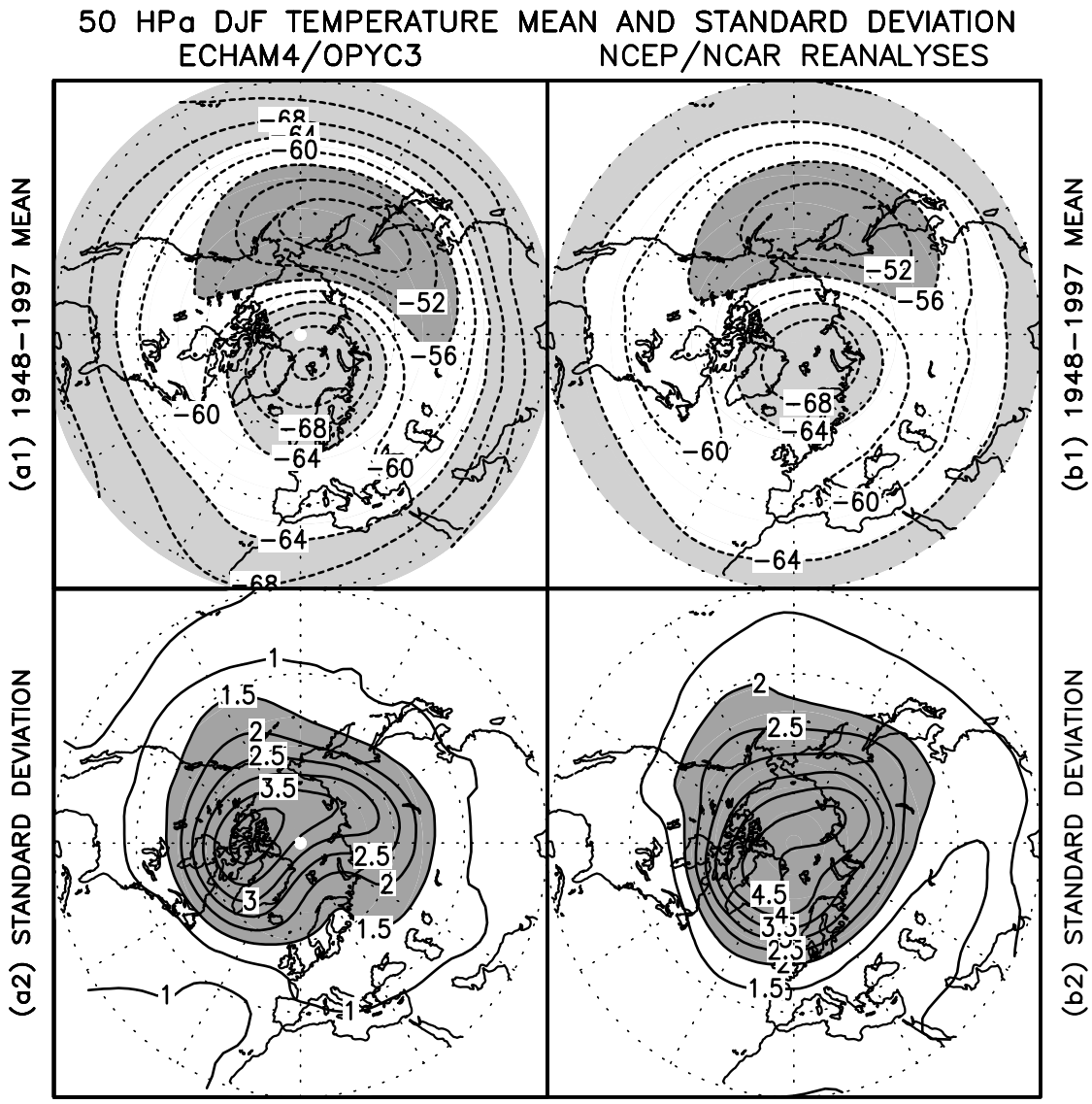

Figure 1: (a1): DJF mean of the temperature at 50 hPa averaged for 50 years (1948-1997) of the GHG run of the ECHAM4/OPYC3 model and (a2): the corresponding standard deviations poleward of 20°N. (b1) and (b2) are same as (a1) and (a2), but for the NCEP/NCAR reanalyses of 1948-1997. The contour intervals are 4°C in (a1) and (b1), and 0.5°C in (a2) and (b2). Heavy (light) shaded regions indicate the values larger (less) than -56°C (-64°C) in (a1) and (b1), and larger than 1.5°C in (a2) and 2.0°C in (b2).

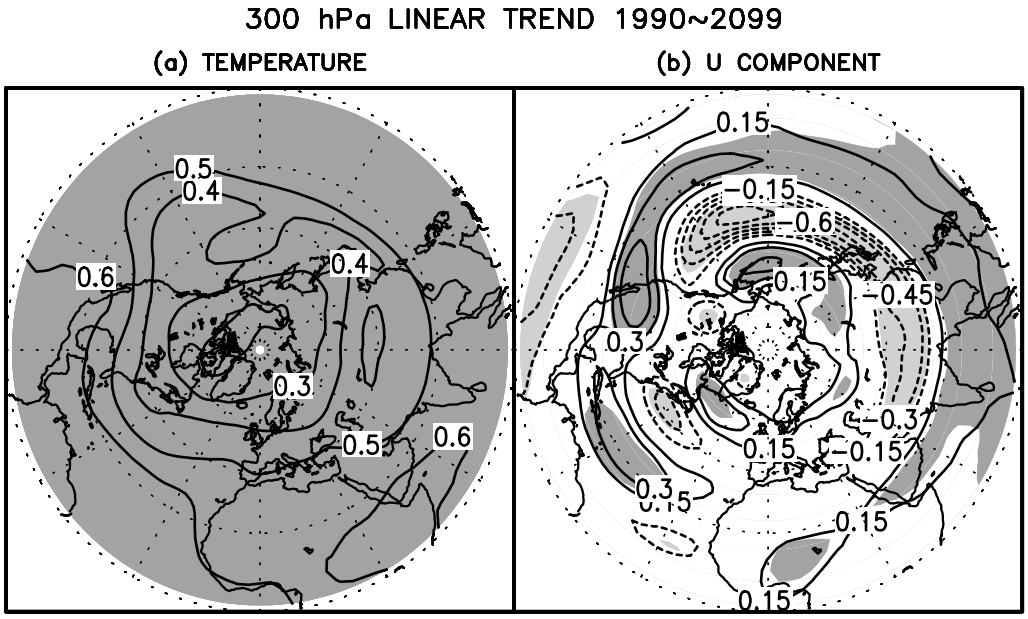

Figure 2: Linear trends of the temperature (a) and U component (b) at 300 hPa in the NH winter during the period from the year 1990 to the year 2100. The contour intervals are 0.1°C/decade in (a) and 0.15 m/s/decade in (b). Solid (dashed) lines represent positive (negative) values. Heavy (light) shaded regions indicate the positive (negative) trends significant at the level of 95% using the T-test.

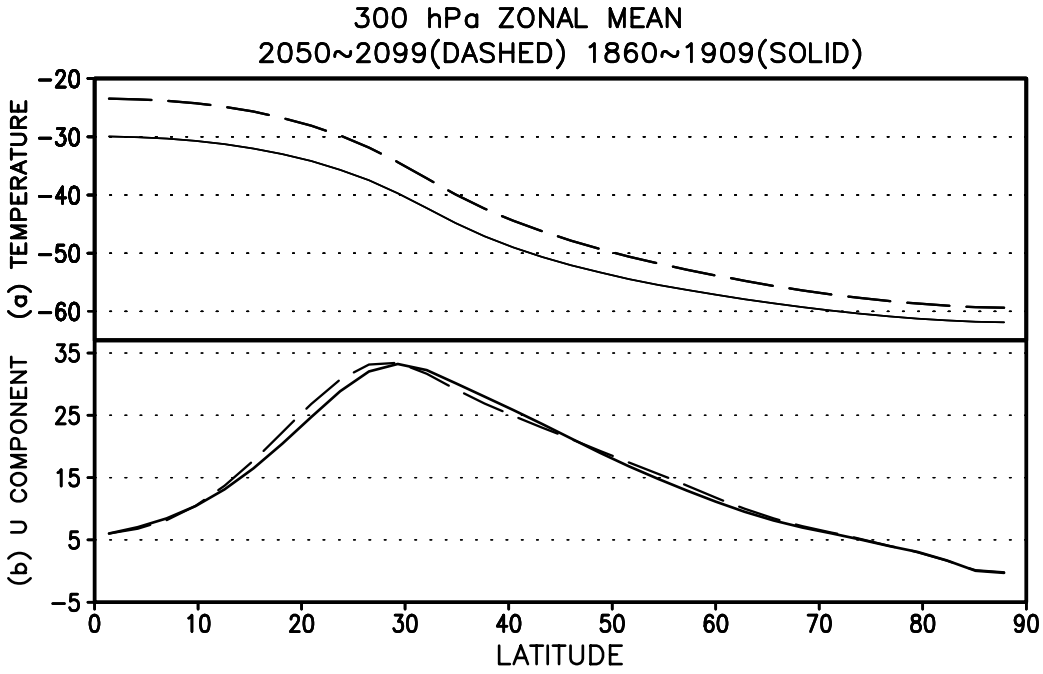

Figure 3: Latitude-variation of zonal mean of the temperature (a) and U component (b) at 300 hPa in the NH averaged for the period of 1860-1910 (solid lines) and 2050-2100 (dashed lines) in winter. The units are °C in (a) and m/s in (b).

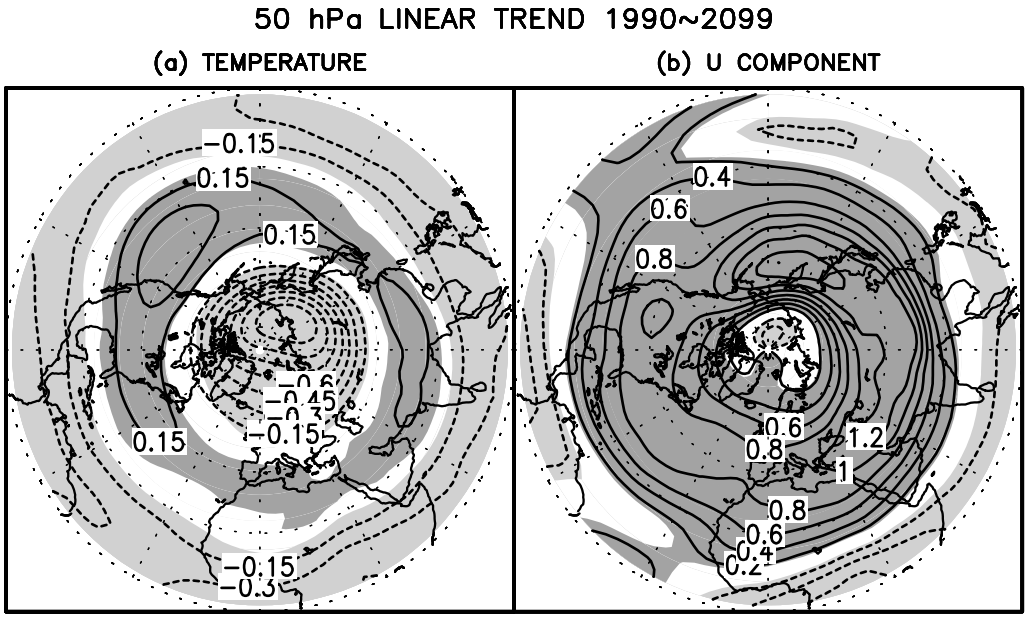

Figure 4: Same as Figure 2 but for the temperature (a) and U component (b) at 50 hPa. The contour intervals are 0.15°C/decade in (a) and 0.2 m/s/decade in (b).

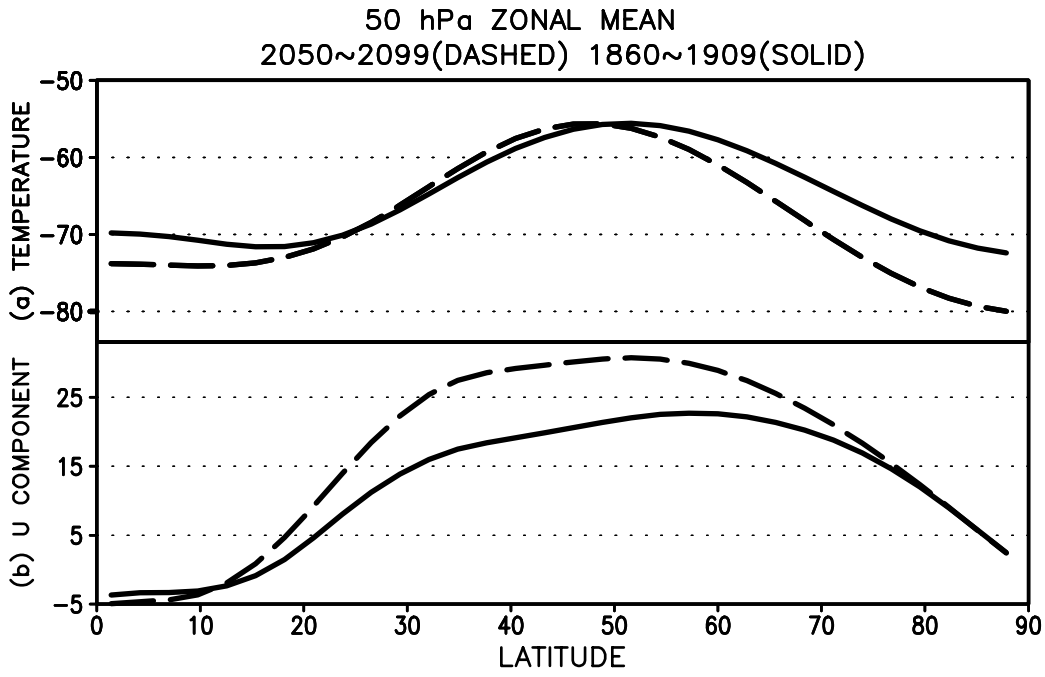

Figure 5: Same as Figure 3 but for the temperature (a) and U component (b) at 50 hPa.

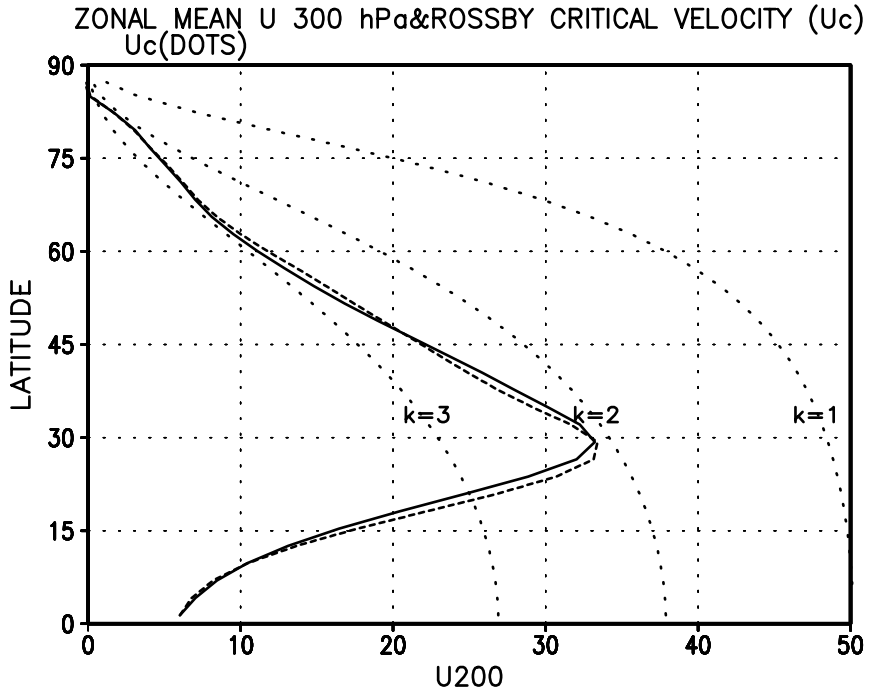

Figure 6: The dotted lines represent the Rossby critical velocity (Uc) for meridional wave number l=0 and zonal wave number k=1, 2, 3, respectively. The solid lines and dashed lines are repeated from Figure 3b, which are the zonal mean of the U component of wind at 300 hPa in the NH winter averaged for the periods of 1860-1910 and 2050-2100, respectively. The unit is m/s

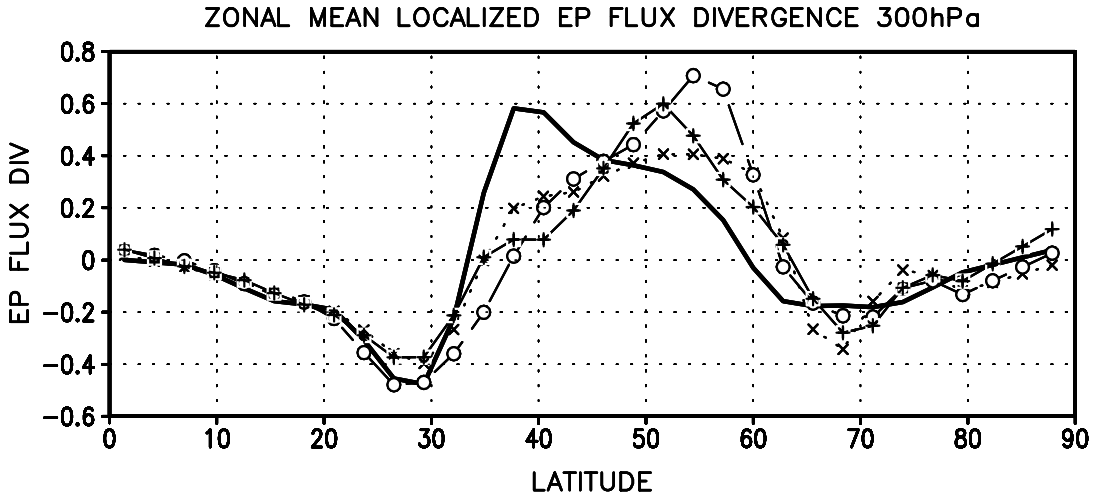

Figure 7: Zonal mean localized Eliassen-Palm flux divergence at 300 hPa in winter for the decadal averages in the periods of 1980-1990 (solid line), 2030-2040 (line with x), 2070-2080 (line with o), and 2090-2100 (line with +). The unit is m/s/day.

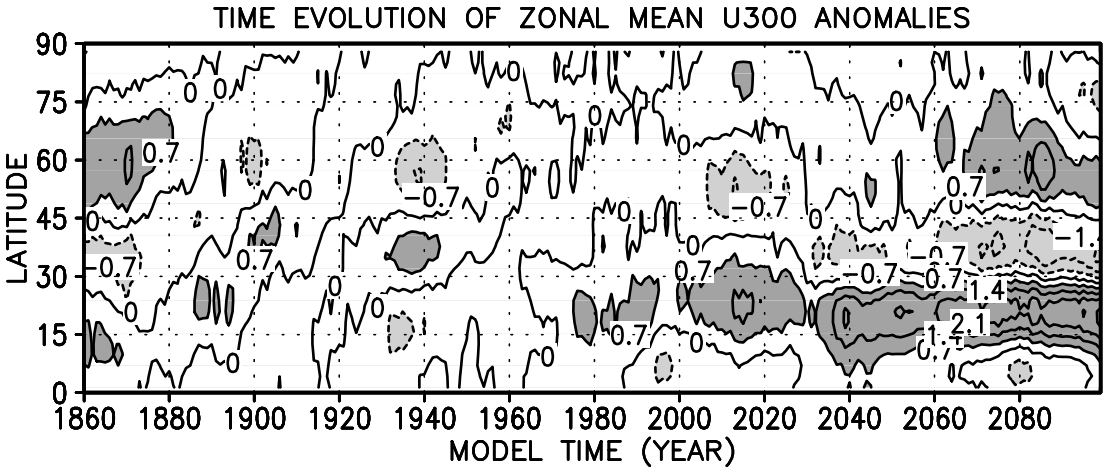

Figure 8: Time-evolution of zonal mean of the zonal component of wind anomalies at 300 hPa in winter. The anomalies are calculated relative to the mean of 1860-1980. The contour interval is 0.7 m/s. Solid (dashed) lines represent positive (negative) values. Heavy (light) shaded regions indicate the values larger (less) than 0.7 (-0.7) m/s